

# Performance Evaluation and Analysis of Three Pin Constant Velocity Joint

Rajkumar Nandkumar Patil

**Abstract**—Presently Oldham’s coupling and Universal joints are used for parallel offset power transmission and angular offset transmission. The basic function of a power transmission coupling is to transmit torque from an input shaft to an output shaft at a given shaft speed and where necessary to accommodate shaft misalignment. These joints have limitations on maximum offset distance / angle /speed and result in vibrations and low efficiency (below 70%). The three pin constant velocity joint is an alteration in design that offers up to 15 mm parallel offset and 12 degree angular offset, at high speeds up to 2000 or 2500 rpm @ 90% efficiency. This design lowers cost of production, space requirement and simply technology of manufacture as compared to present CVJ in market.

**Index Terms**—3-pin Constant Velocity Joint, Angular Offset, Parallel Offset, Power Transmission, Von-Mises Stress

## I. INTRODUCTION

A coupling is a device used to connect two shafts together at their ends for the purpose of transmitting power. Couplings do not normally allow disconnection of shafts during operation, however there are torque limiting couplings which can slip or disconnect when some torque limit is exceeded.

The primary purpose of couplings is to join two pieces of rotating equipment while permitting some degree of misalignment or end movement or both. By careful selection, installation and maintenance of couplings, substantial savings can be made in reduced maintenance costs and downtime.

The Thomson constant velocity joint is a constant velocity joint with no parasitic bearing of sliding surfaces. This invention offers a revolution in the design of many transmission system, for instance in vehicular, marine, manufacturing, industrial and aeronautical application.

It is essentially two cardan joints assembled co-axially where the cruciform-equivalent members of each are

connected to one another by trunions and bearings which are constrained to continuously lie on the homokinetic plane of the joint.

## II. LITERATURE REVIEW

**A. Ian Watson, B. Gangadhara Prusty and John Olsen** have stated in research paper titled “Conceptual design optimization of a constant velocity coupling” that The Thompson Coupling operates using the robust double Cardan mechanism. Constant velocity and determinate linkage kinematics are maintained by a spherical pantograph. This mechanism forms an extra loop attached to the intermediate shaft in the double Cardan linkage, and consequently constrains this shaft to bisect the axis of input and output. Closed-form expressions for its motion and the rotation of the double Cardan joint are derived by consideration of spherical linkage kinematics. These expressions are then used to drive basic conceptual design optimization, whose goal is to reduce induced driveline vibration. The findings of this optimization are discussed with respect to the current design of the Thompson joint. Improvements in induced driveline vibration are possible, subject to the satisfaction of other coupling design criteria.

**B. Chul-Hee Lee and Andreas A. Polycarpou** has proposed in their research paper titled “A phenomenological friction model of tripod constant velocity (CV) joints” that constant velocity (CV) joints have been favored for automotive applications, compared to universal joints, due to their superiority of constant velocity torque transfer and plunging capability. High speed and sport utility vehicles with large joint articulation angles, demand lower plunging friction inside their CV joints to meet noise and vibration requirements, thus requiring a more thorough understanding of their internal friction characteristics. A phenomenological CV joint friction model was developed to model the friction behavior of tripod CV joints by using an instrumented CV joint friction apparatus with tripod-type joint assemblies. Experiments were conducted under different operating conditions of oscillatory speeds, CV joint articulation angles, lubrication, and torque. The experimental data and physical parameters were used to develop a physics-based phenomenological CV joint dynamic friction model. It was

Manuscript received November 17, 2017.

Rajkumar Nandkumar Patil has completed B.E. from Government College of Engineering and Research, Awasari, Pune, 412405 INDIA. He is Mechanical Engineer  
(email: prajkumar308@gmail.com)

found that the proposed friction model captures the experimental data well, and the model was used to predict the external generated axial force, which is the main source of force that causes vehicle vibration problems.

**C. Majid Yaghoubi, Seyed Saeid Mohtasebi, Ali Jafary and Hamid Khaleghi** in their research work titled “Design, manufacture and evaluation of a new and simple mechanism for transmission of power between intersecting shafts up to 135 degrees (Persian Joint)” has introduced a new mechanism which is designed for the transmission of power between two intersecting shafts. The mechanism consists of one drive shaft and one driven shaft, six guide arms, and three connecting arms. The intersecting angle between the input shaft and the output shaft can be varied up to 135° while the velocity ratio between the two shafts remains constant. The research also includes a kinematic analysis and a simulation using Visual NASTRAN, Autodesk Inventor Dynamic and COSMOS Motion. The software showed that this mechanism can transmit constant velocity ratios at all angles between two shafts. By comparing the graphs of analytical analysis and simulation analysis, validity of equations was proved.

**D. Katsumi Watanabe and Takashi Matsuura** in their research paper titled “Kinematic Analyses of Rzeppa Constant Velocity Joint by Means of Bilaterally Symmetrical Circular-Arc-Bar Joint” has proposed that mechanism whose elements are bilaterally symmetrical with respect to the bisecting plane of driving and driven rotational axes is able to use as the constant velocity joint. The constant velocity joint that is composed of input and output shafts, two circular-arc elements and the frame is a most elementary joint. The closed loop equation of the circular-arc-bar joint whose kinematic constants are any values is deduced in the form of the quadratic equation of the output angle. The Rzeppa constant velocity joint is composed of several sets of the ball and two circular-arc grooves. A relative motion of the ball to two circular-arc grooves is analyzed and the output angle error in a practical use which contains sinusoidal fluctuations with periods  $2\pi$ ,  $2\pi/3$ , and  $2\pi/6$  is simulated by the circular-arc-bar constant velocity joint.

**E. Tae-Wan Ku, Lee-Ho Kim and Beom-Soo Kang** in their research work titled “Multi-stage cold forging and experimental investigation for the outer race of constant velocity joints” has explored that as an important load-supporting automobile part that transmits torque between the transmission and the driven wheel, the outer race of CV (constant velocity) joints with six inner ball grooves has been conventionally produced by the multi-stage warm forging processes, which involves several operations including forward extrusion, upsetting, backward extrusions,

sizing and necking, as well as additional machining. There is still no choice but to produce the complex shaped components other than by this warm forging process. As an alternative, multi-stage cold forging process is presented to replace these traditional warm forging. The multi-stage cold forging procedure is first considered through a process assessment regarding the traditional multistage warm forging one. Then, the process is simplified and redesigned as one operation to produce the forged outer race and the backward extrusions of the traditional process, and the sizing and necking are also combined into a single sizing necking process.

### III. SYSTEM DESIGN

#### A) Design Considerations

In system design we mainly concentrated on the following parameters: -

##### 1. System Selection Based on Physical Constraints

While selecting any machine it must be checked whether it is going to be used in a large-scale industry or a small-scale industry. In our case it is to be used by a small-scale industry. So space is a major constrain. The system is to be very compact so that it can be adjusted to corner of a room. The mechanical design has direct norms with the system design. Hence the foremost job is to control the physical parameters, so that the distinctions obtained after mechanical design can be well fitted into that.

##### 2. Arrangement of Various Components

Keeping into view the space restrictions the components should be laid such that their easy removal or servicing is possible. More over every component should be easily seen none should be hidden. Every possible space is utilized in component arrangements.

##### 3. Components of System

As already stated the system should be compact enough so that it can be accommodated at a corner of a room. All the moving parts should be well closed & compact. A compact system design gives a high weighted structure which is desired.

##### 4. Man Machine Interaction

The friendliness of a machine with the operator that is operating is an important criteria of design. It is the application of anatomical & psychological principles to solve problems arising from Man – Machine relationship.

##### 5. Chances of Failure

The losses incurred by owner in case of any failure is an important criteria of design. Factor safety while doing

mechanical design is kept high so that there are less chances of failure. Moreover periodic maintenance is required to keep unit healthy.

### 6. Servicing Facility

The layout of components should be such that easy servicing is possible. Especially those components which require frequent servicing can be easily disassembled.

### 7. Height of Machine from Ground

For ease and comfort of operator the height of machine should be properly decided so that he may not get tired during operation. The machine should be slightly higher than the waist level, also enough clearance should be provided from the ground for cleaning purpose.

### 8. Weight of Machine

The total weight depends upon the selection of material components as well as the dimension of components. A higher weighted machine is difficult in transportation & in case of major breakdown, it is difficult to take it to workshop because of more weight..

### B) Selection of Motor

The metric system uses kilowatts (kW) for driver ratings. Converting kW to torque:

$$T = kW \times 84518 \text{ rpm}$$

Where

T = the torque in inch pounds

KW the motor or other kilowatts

rpm = the operating speed in revolutions per minute

84518 = a constant used when torque is in inch-pounds. Use

7043 for foot-pounds, and 9550 for Newton-meters

$$0.3 = kW \times 9550 / 1200$$

$$kW = 0.038 \text{ kW}$$

Thus the minimum input power required will be 38 watt.

### Drive Motor

Type: - Single Phase Ac Motor.

Power: - 1 /15 Hp. (50 Watts)

Voltage: - 230 Volts, 50 Hz

Current: - 0.5 Amps

Speed: - Min = 0 rpm, Max = 9500 rpm

TEFC Construction, Commentator Motor.

### C) Design of Belt Drive

Power is transmitted from the motor shaft to the input shaft of drive by means of an open belt drive,

Motor pulley diameter = 20 mm

Input shaft pulley diameter = 100 mm

Reduction ratio = 5

Input shaft speed = 9500/5 = 1900 rpm

T motor = 0.05 Nm

Torque at Input shaft = 5 x 0.05 = 0.25 Nm

### 1. Design of Open Belt Drive

Motor pulley diameter = 20 mm

Input shaft pulley diameter = 110 mm

Reduction ratio = 5

Coefficient of friction = 0.23

Maximum allowable tension in belt = 200 N

Center distance = 120

Wrap angle of pulley

$$\alpha = 180 - 2\sin^{-1} [(D-d)/2C]$$

$$\alpha = 180 - 2\sin^{-1} [(110-20) / (2 \times 120)]$$

$$\alpha = 136^\circ$$

$$\alpha = 2.37^\circ$$

Now,

$$e^{\mu\alpha/\sin(\theta/2)} = e^{0.2 \times 2.37 \sin(40/2)} = 4$$

Width (b<sub>2</sub>) at base is given by

$$b_2 = 6 - 2(4 \tan 20) = 3.1$$

Area of cross section of belt = 1/2{6 + 3.1} x 4

$$A = 18.2 \text{ mm}^2$$

Now mass of belt /m length = 0.23 kg/m

$$V = \pi DN / (60 \times 1000) = 4.188 \text{ m/sec}$$

$$T_c = m V^2$$

$$T_c = 4.034 \text{ N}$$

T<sub>1</sub> = Maximum tension in belt – T<sub>c</sub>

$$T_1 = 195.966 = 196 \text{ N}$$

$$T_1 / T_2 = e^{\mu\alpha/\sin(\theta/2)} = 4$$

$$T_2 = 49 \text{ N}$$

### 2. Result

Tension in tight side of belt (T<sub>1</sub>) = 196 N

Tension in slack side of belt (T<sub>2</sub>) = 49 N

### D) Design of Input and Output Shaft

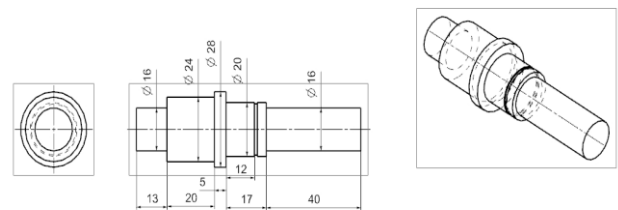


Fig. 1. Design of input and output shaft

### 1. Material Selection

TABLE I: MATERIAL SELECTION OF SHAFT

Designation	Ultimate Tensile Strength N/mm <sup>2</sup>	Yield Strength N/mm <sup>2</sup>
EN 24	800	680

$$f_{s \max} = UTS / FOS = 800 / 2 = 400 \text{ N/mm}^2$$

This is the allowable value of shear stress that can be induced in the shaft material for safe operation.

Check for torsional shear failure of shaft.

$$T_e = \frac{\pi f_s d^3}{16}$$

$$f_{s \text{ act}} = \frac{16 \times 0.25 \times 10^3}{\pi \times 16^3}$$

$f_{b \text{ act}} = 0.310 \text{ N/mm}^2$ , As;  $f_{s \text{ act}} < f_{s \text{ all}}$   
Shaft is safe under torsional load.

## 2. Ansys Model

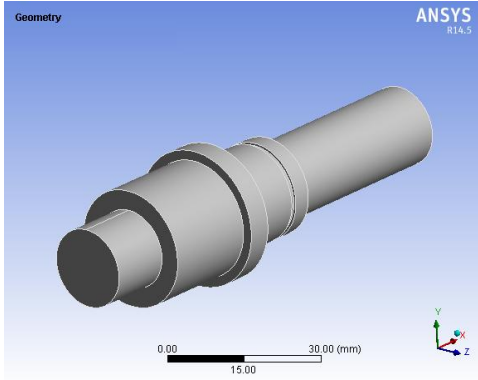


Fig. 2. Geometry of Shaft

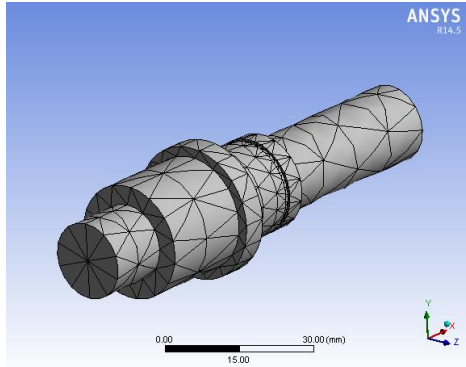


Fig. 3. Meshing of Shaft

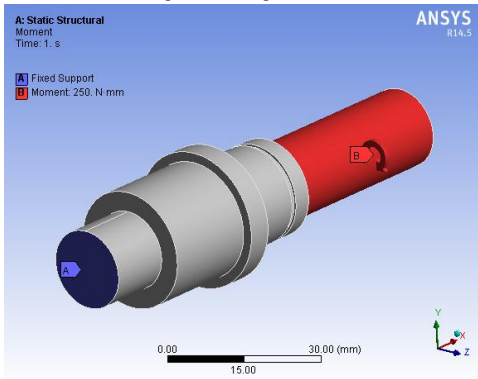


Fig. 4. Boundary Conditions of Shaft

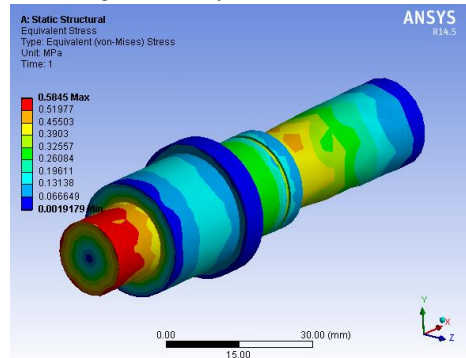


Fig. 5. Von-mises stress of Shaft

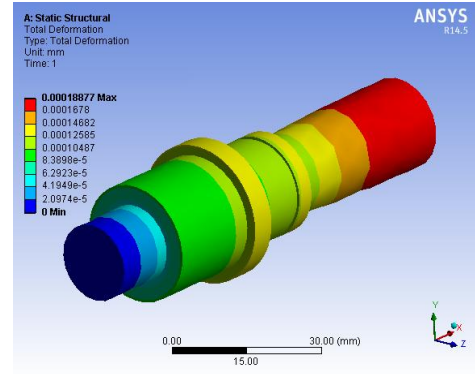


Fig. 6. Total Deformation of shaft

## 3. Result & discussion

TABLE 2: RESULT TABLE FOR SHAFT

Part Name	Maximum theoretical stress N/mm <sup>2</sup>	Von-mises stress N/mm <sup>2</sup>	Total deformation Mm	Result
Input Shaft	0.310	0.5845	0.0001887	Safe

## 4. Conclusion.

- Maximum stress by theoretical method and Von-mises stress are well below the allowable limit, hence the input shaft is safe.
- Shaft shows negligible deformation.

## E) Design of Input and Output Coupler Body

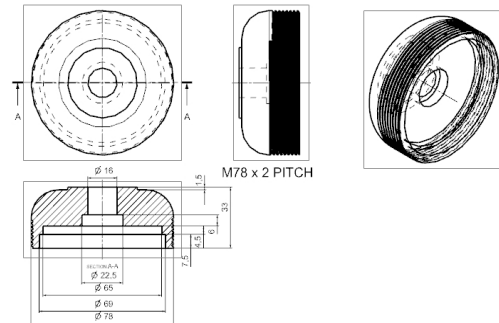


Fig. 7. Design of coupler body

## 1. Material Selection.

TABLE 3: MATERIAL SELECTION OF COUPLER BODY

Designation	Ultimate N/mm <sup>2</sup>	Tensile strength	Yield strength N/mm <sup>2</sup>
Aluminium	400		280

$$f_{s \text{ max}} = \text{UTS}/\text{FOS} = 400/2 = 200 \text{ N/mm}^2$$

Check for torsional shear failure:-

$$T = \frac{\pi \times f_{s \text{ act}} \times \left( \frac{D_o^4 - D_i^4}{D_o} \right)}{16}$$

$$0.25 \times 10^3 = \frac{\pi \times f_{s \text{ act}} \times \left( \frac{22.5^4 - 16^4}{22.5} \right)}{16}$$

$$f_{s \text{ act}} = 0.15 \text{ N/mm}^2$$

$$As; fs_{act} < fs_{all}$$

Input coupler body is safe under torsional load.

## 2. Ansys Model

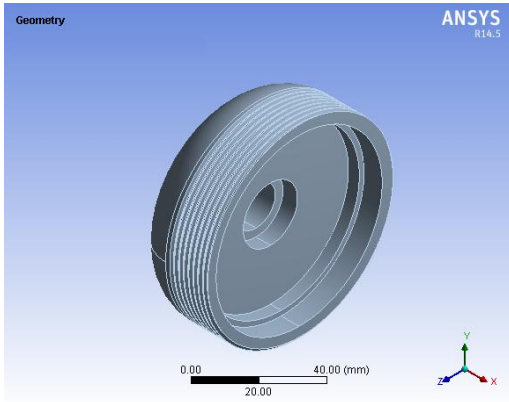


Fig.8. .Geometry of coupler body

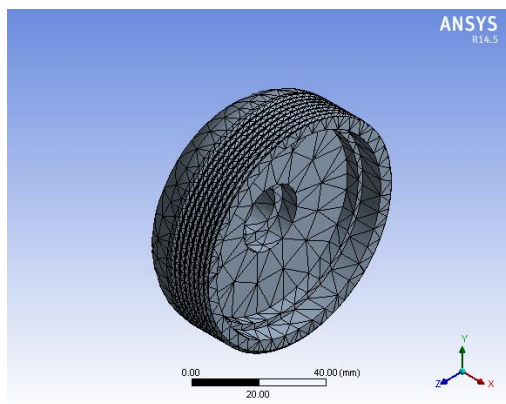


Fig. 9 .Meshing of coupler body

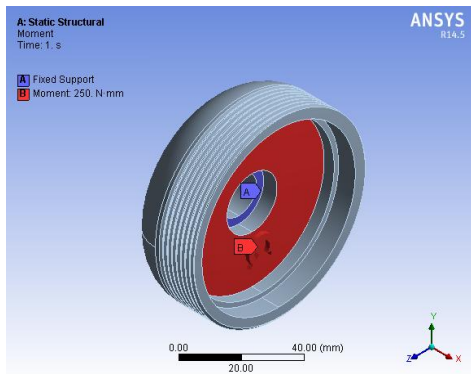


Fig. 10. Boundary Conditions of coupler body

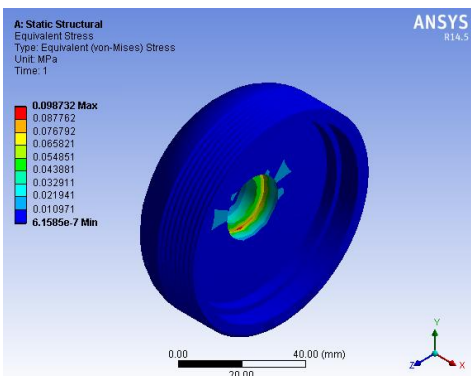


Fig. 11. Von-mises stress of coupler body

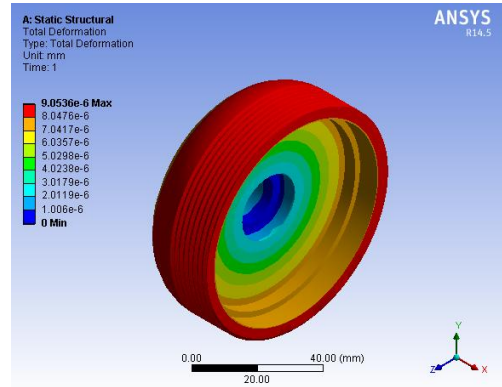


Fig 12. Total Deformation of coupler body

## 3. Result & Discussion

TABLE 4: RESULT TABLE FOR COUPLER BODY

Part Name	Maximum theoretical stress N/mm <sup>2</sup>	Von-mises stress N/mm <sup>2</sup>	Total defn Mm	Result
Input Coupler Body	0.15	0.098	9.06E-6	Safe

## 4. Conclusion.

a) Maximum stress by theoretical method and Von-mises stress are well below the allowable limit, hence the input coupler body is safe.

## F) Design of Input and Output Coupler Ring

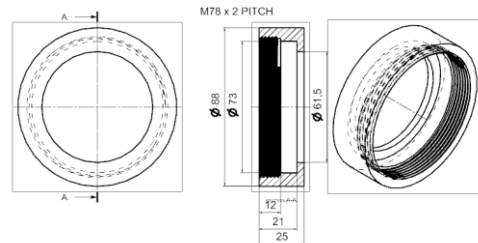


Fig. 13. Design of coupler ring

## 1. Material Selection.

TABLE 5: MATERIAL SELECTION FOR COUPLER RING

Designation	Ultimate Tensile strength N/mm <sup>2</sup>	Yield strength N/mm <sup>2</sup>
EN 24	800	680

$$fs_{max} = 400N/mm^2$$

Check for torsional shear failure:-

$$T = \frac{\Pi \times fs_{act} \times \left( \frac{Do^4 - Di^4}{Do} \right)}{16}$$

$$0.25 \times 10^3 = \frac{\Pi \times fs_{act} \times \left( \frac{88^4 - 73^4}{88} \right)}{16}$$

$$fs_{act} = 0.0035/mm^2$$

$$As; fs_{act} < fs_{all}$$

Input Coupler ring is safe under torsional load

## 2. Ansys Model

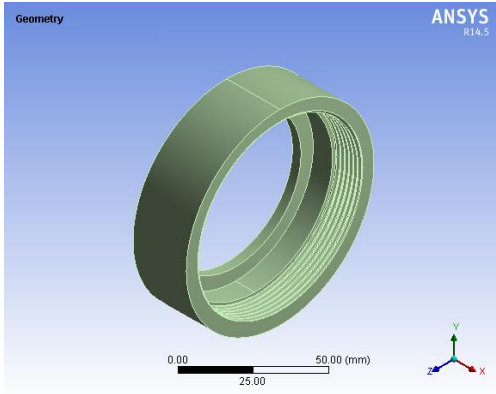


Fig. 14. .Geometry of coupler ring

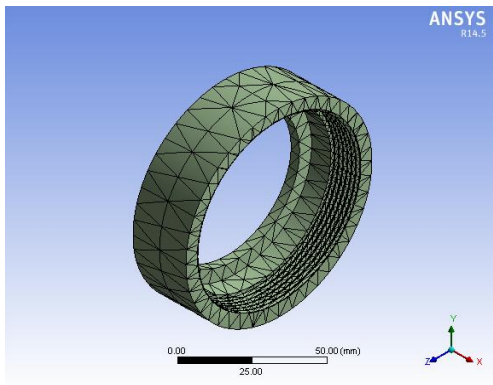


Fig. 15. .Meshing of coupler ring

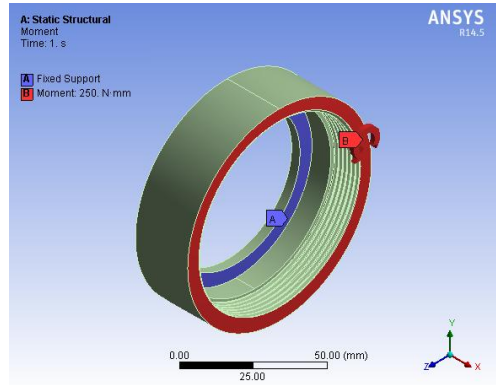


Fig. 16.. Boundary Conditions of coupler ring

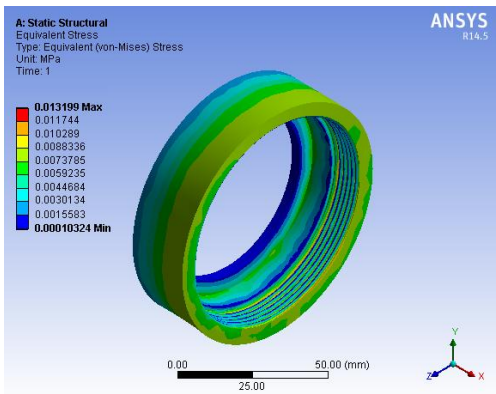


Fig. 17. Von-mises stress of coupler ring

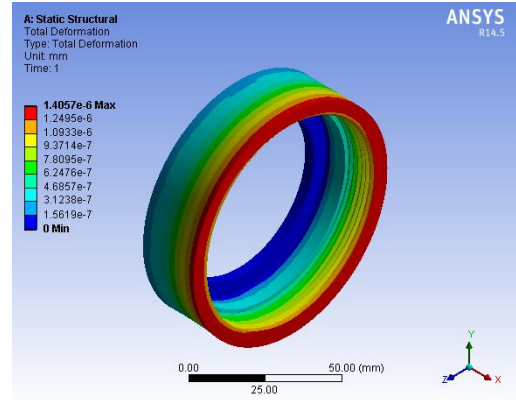


Fig.18. Total Deformation of coupler ring

## 3. Result & discussion

TABLE 6: RESULT TABLE FOR COUPLER RING

Part Name	Maximum theoretical stress N/mm <sup>2</sup>	Von-mises stress N/mm <sup>2</sup>	Total def. Mm	Result
Input Coupler Ring	0.0035	0.013	1.045E-6	safe

## 4. Conclusion.

- Maximum stress by theoretical method and Von-mises stress are well below the allowable limit, hence the input coupler ring is safe.
- Input coupler ring shows negligible deformation.

## G) Selection of Ball Bearing for Input and Output Shaft; Selection of bearing 6004 ZZ

The input shaft is held in two ball bearings that equally share the radial load on the shaft. Selecting; Single Row deep groove ball bearing as follows.

Series 60

TABLE 7: BEARING DATA (6004)

ISl No	Bearing of basic design No (SKF)	D	D1	D	D <sub>2</sub>	B	Basic capacity	
2AC04	6004	20	23	42	36	12	450 0	73 50

$$P = X F_r + Y F_a$$

Neglecting self-weight of carrier and gear assembly

For our application  $F_a = 0$

$$P = X F_r$$

$$\text{Where } F_r = P_t = T_1 + T_2 = 196 + 49 = 245 \text{ N}$$

$$\text{Max radial load} = F_r = 245 \text{ N.}$$

$$P = 145 \text{ N}$$

Calculation dynamic load capacity of bearing.

$$L = (C / P)^p, \text{ where } p = 3 \text{ for ball bearings.}$$

For m/c used for eight hr of service per day;

$$L_H = 4000 - 8000 \text{ hr}$$

$$\text{But; } L = 60 n L_H / 10^6$$



$L = 60 \times 1900 \times 4000 / 10^6$  mrev ....here speed of shaft is considered to be 1900 rpm

$L = 456$

$$\text{Now; } 456 = \frac{(C)^3}{(145)^3}$$

$C = 1885 \text{ N}$

As the required dynamic capacity of bearing is less than the rated dynamic capacity of bearing;

Bearing is safe.

### H) Design of Input and output Coupler Female Liner

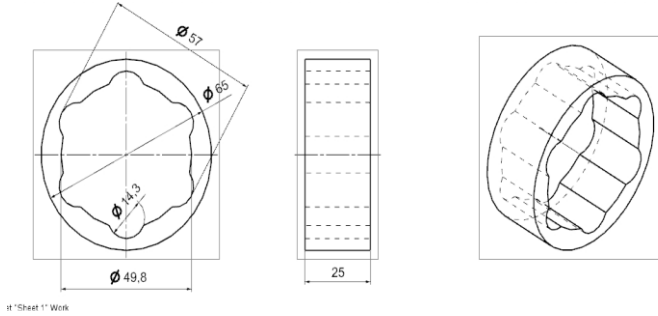


Fig.19 Design of coupler female liner

### 1. Material Selection.

TABLE 8: MATERIAL SELECTION OF COUPLER FEMALE LINER

Designation	Ultimate Tensile strength N/mm <sup>2</sup>	Yield strength N/mm <sup>2</sup>
EN 24	800	680

$$f_{s \max} = 400 \text{ N/mm}^2$$

Check for torsional shear failure:-

$$T = \frac{\pi \times f_{s \text{ act}} \times D_o^4 - D_i^4}{16 D_o}$$

$$0.25 \times 10^3 = \frac{\pi \times f_{s \text{ act}} \times (65^4 - 57^4)}{16 \times 65}$$

$$f_{s \text{ act}} = 0.0113 \text{ N/mm}^2$$

As;  $f_{s \text{ act}} < f_{s \text{ all}}$

Input Coupler female liner is safe under torsional load.

### 2. Ansys Model

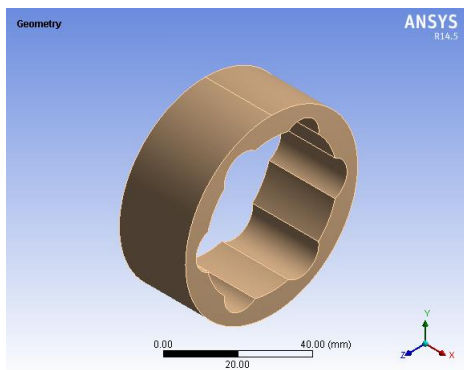


Fig. 20. Geometry of coupler female liner

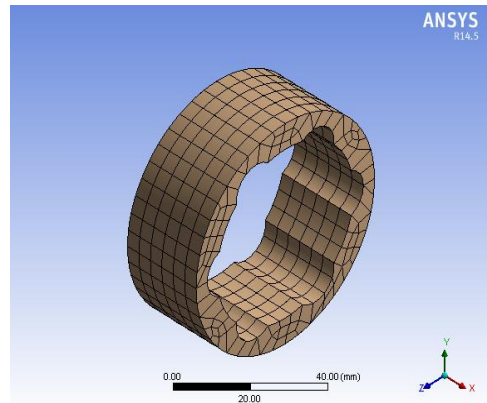


Fig. 21. Meshing of coupler female liner

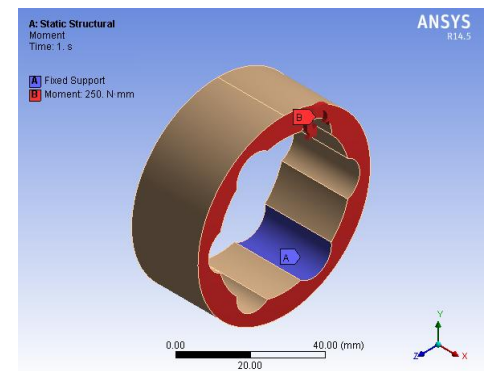


Fig. 22. Boundary Conditions of coupler female liner

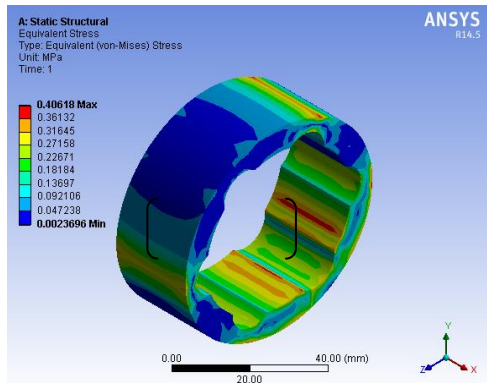


Fig. 23. Von-mises stress of coupler female liner

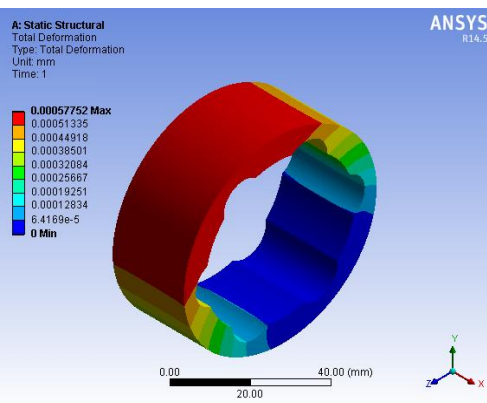


Fig.24 Total Deformation of coupler female liner

### 3. Result & discussion

TABLE 9: RESULT TABLE FOR COUPLER FEMALE LINER

Part Name	Maximum theoretical stress N/mm <sup>2</sup>	Von-mises stress N/mm <sup>2</sup>	Total deformation mm	Result
Input coupler female liner	0.0113	0.40	1.045E-6	Safe

### 4. Conclusion.

- Maximum stress by theoretical method and Von-mises stress are below the allowable limit, hence ring is safe.
- Input coupler ring shows negligible deformation

### 1) Design of Coupler Pin

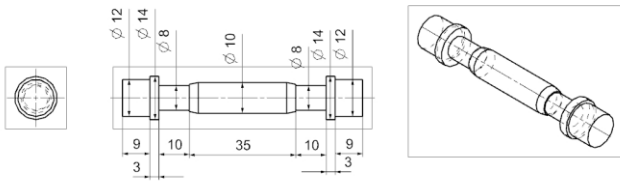


Fig 25: Design of coupler pin

### 1. Material Selection.

TABLE 10: MATERIAL SELECTION OF COUPLER PIN

Designation	Ultimate Tensile strength N/mm <sup>2</sup>	Yield strength N/mm <sup>2</sup>
EN 24	800	680

$$f_{s \max} = \frac{uts}{fos} = \frac{800}{2} = 400 \text{ N/mm}^2$$

This is the allowable value of shear stress that can be induced in the shaft material for safe operation.

Check for torsional shear failure of shaft

$$T_e = \frac{\Pi}{16} f_s d^3$$

$$f_{s \text{ act}} = \frac{16 \times 0.25 \times 10^3}{\Pi \times 8^3}$$

$$f_{b \text{ act}} = 2.4860 \text{ N/mm}^2, \text{ As; } f_{s \text{ act}} < f_{s \text{ all}}$$

Coupler pin is safe under torsional load.

### 2. Ansys Model

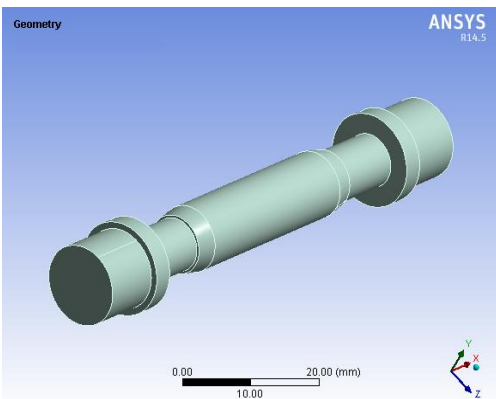


Fig. 26.Geometry of coupler pin

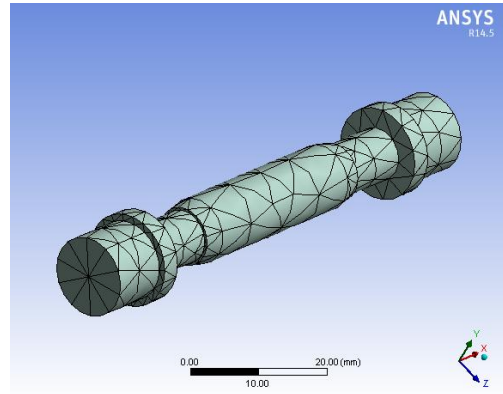


Fig. 27.Meshing of coupler pin

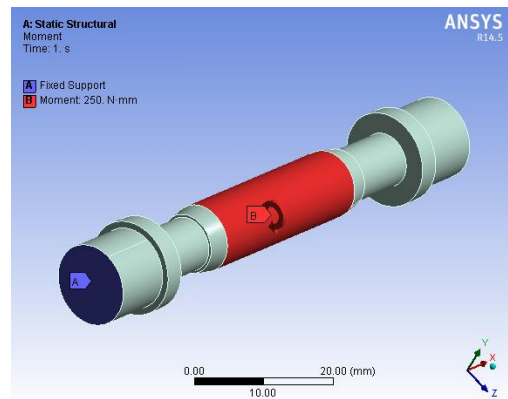


Fig. 28. Boundary Conditions of coupler pin

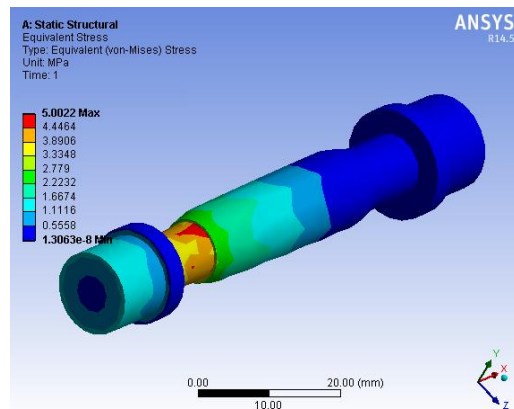


Fig. 29. Von-mises stress of coupler pin

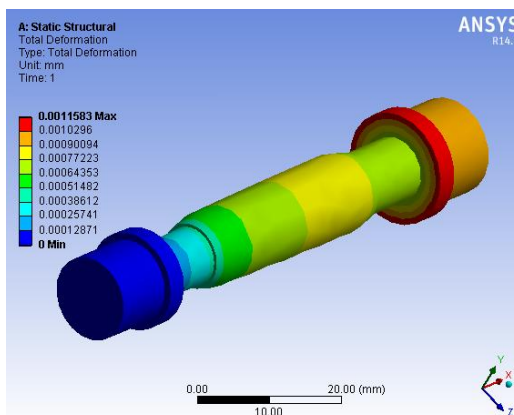


Fig.30 Total Deformation of coupler pin



### 3. Result & discussion

TABLE 11: RESULT TABLE FOR COUPLER PIN

Part Name	Maximum theoretical stress N/mm <sup>2</sup>	Von-mises stress N/mm <sup>2</sup>	Total deformation Mm	Result
Coupler pin	2.486	5.02	0.0011	Safe

### 4. Conclusion.

- a) Maximum stress by theoretical method and Von-mises stress are well below the allowable limit, hence the coupler pin is safe.
- b) Coupler pin shows negligible deformation.

### J) Design of Trunion Holder

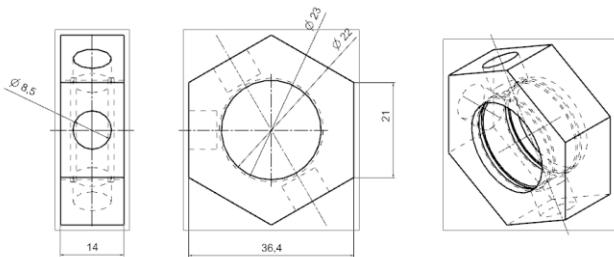


Fig. 31 Design of trunion holder

### 1. Material Selection.

TABLE 12: MATERIAL SELECTION FOR TRUNION HOLDER

Designation	Ultimate Tensile strength N/mm <sup>2</sup>	Yield strength N/mm <sup>2</sup>
Aluminium	400	280

$$f_{s \max} = UTS/FOS = 400/2 = 200 \text{ N/mm}^2$$

Check for torsional shear failure:-

$$T = \frac{\pi \times f_{s \text{ act}} \times \left( \frac{D_o^4 - D_i^4}{D_o} \right)}{16}$$

$$0.25 \times 10^3 = \frac{\pi \times f_{s \text{ act}} \times \left( \frac{36.4^4 - 23^4}{36.4} \right)}{16}$$

$$f_{s \text{ act}} = 0.2 \text{ N/mm}^2$$

As;  $f_{s \text{ act}} < f_{s \text{ all}}$

Trunion holder is safe under torsional load.

### 2. Ansys Model

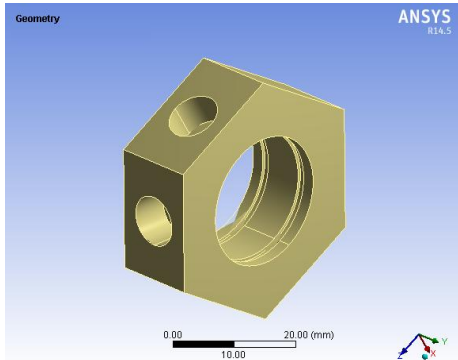


Fig. 32. Geometry of trunion holder

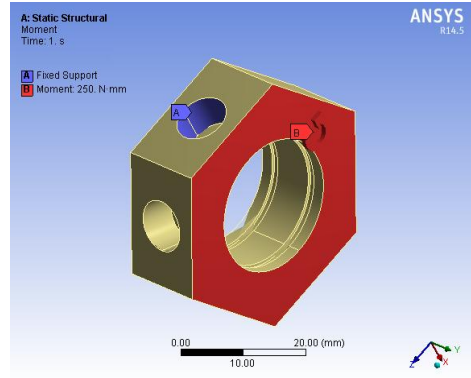


Fig. 33. Boundary Conditions of trunion holder

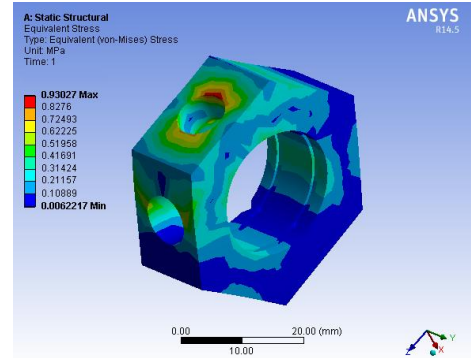


Fig. 34. Von-mises stress of trunion holder

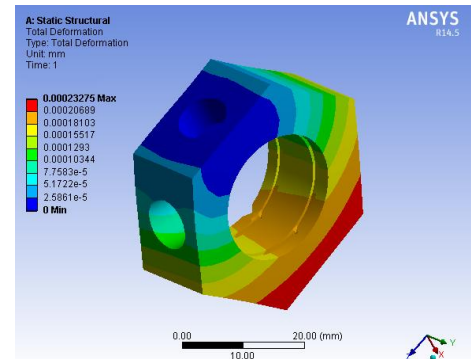


Fig. 35. Total Deformation of trunion holder

### 3. Result & discussion

TABLE 13: RESULT TABLE FOR TRUNION HOLDER

Part Name	Maximum theoretical stress N/mm <sup>2</sup>	Von-mises stress N/mm <sup>2</sup>	Total deformation Mm	Result
Trunion holder	0.2	0.9	0.00023	Safe

### 4. Conclusion.

- a) Maximum stress by theoretical method and Von-mises stress are well below the allowable limit, hence the trunion holder is safe.
- b) Trunion holder shows negligible deformation.

## IV. ASSEMBLY

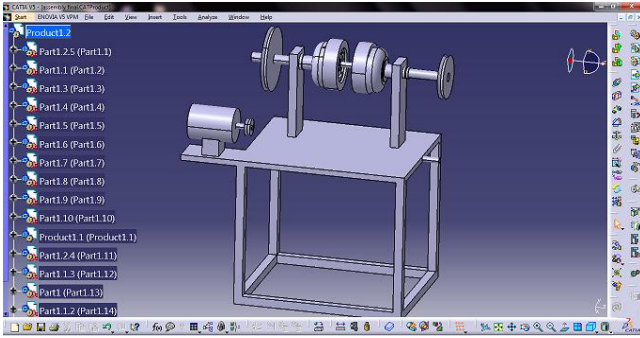


Fig. 36. Actual setup Diagram



Fig. 37. Actual setup Diagram

### 2. Procedure:

- Start motor.
- Let mechanism run & stabilize at certain speed (say 1500 rpm).
- Place the pulley cord on dynamo brake pulley and add 0.1 Kg weight into, the pan, note down the output speed for this load by means of tachometer.
- Add another 0.1 Kg cut & take reading.
- Tabulate the readings in the observation table.
- Plot Torque vs. speed characteristic.
- Plot Power vs. speed characteristic..

### 3. Experimental setup

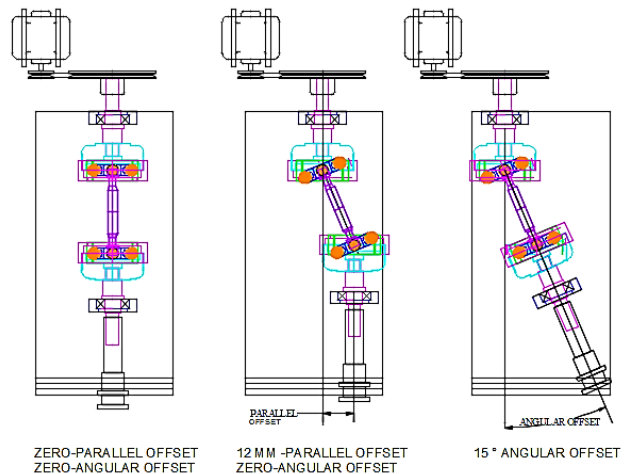


Fig. 39. Experimental setup Diagram

### 4. Observation Table

TABLE 14: OBSERVATION TABLE FOR PARALLEL OFFSET

Sr. NO	Loading		Unloading		Mean speed
	Weight (KG)	Speed rpm	Weight (KG)	Speed rpm	
01	0.2	1480	2	1460	1470
02	0.4	1400	4	1410	1405
03	0.6	1320	6	1340	1330
04	0.8	1210	8	1190	1200
05	1.0	960	10	920	940

## V. EXPERIMENTAL VALIDATION

### 1. Experimental Setup

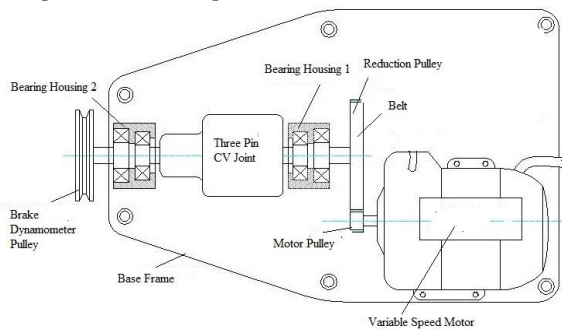


Fig. 38 Setup for three pin constant velocity joint

### Test & Trial

#### A) Coupling Bronze Trunion: Parallel Offset: 12mm

Aim: To conduct trial and plot

- Torque vs. Speed Characteristics
- Power vs. Speed Characteristics

1. Arrangement: In order to conduct trial, a dynamo brake pulley cord, weight pan are provided on the output shaft.

### 5. Sample Calculations :- (At 0.8 Kg Load)

Average speed :-

$$N = \frac{N_1 + N_2}{2} = \frac{1210 + 1190}{2} = 1200 \text{ rpm}$$

Output Torque:-

$$T_{dp} = \text{Weight in pan} \times \text{Radius of Dynamo brake Pulley} \\ = (0.8 \times 9.81) \times 25 \\ = 196.2 \text{ N.mm}$$

$$T_{dp} = 0.1962 \text{ N.m}$$

Input Power :-  $(P_{i/p}) = 29.6 \text{ Watt.}$

Output Power :-  $(P_{o/p})$

$$P_{o/p} = \frac{2 \pi N T_{o/p}}{60}$$

$$= \frac{2 \times \pi \times 0.1962 \times 1200}{60}$$

$$P_{o/p} = 24.6 \text{ watt}$$

Efficiency:-

$$\eta = \frac{\text{Output power}}{\text{Input power}}$$

$$= \frac{24.6}{29.6}$$

$$\eta = 83.10\%$$

Efficiency of transmission of gear drive at 0.8 kg load= 83.10%

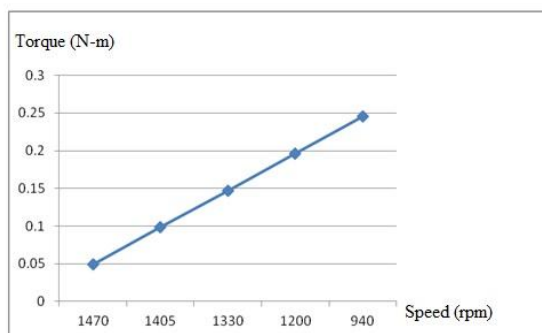
### 6. Result Table

TABLE 15: RESULT TABLE FOR PARALLEL OFFSET

Sr. NO	Load (kg)	Speed (rpm)	Torque (N.M)	Power (watt)	Efficiency
1.	0.2	1470	0.04905	7.55164	25.5123
2.	0.4	1405	0.0981	14.43545	48.7684
3.	0.6	1330	0.14715	20.49731	69.24766
4.	0.8	1200	0.1962	24.65842	83.30546
5.	1.0	940	0.24525	24.1447	81.56993

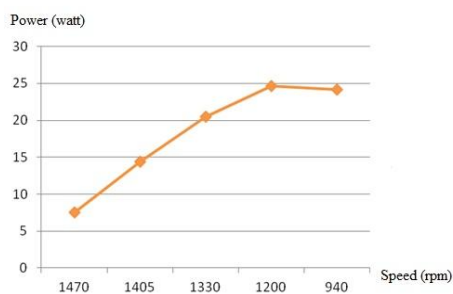
### 7. Characteristics Plots

#### 1) Torque vs Speed



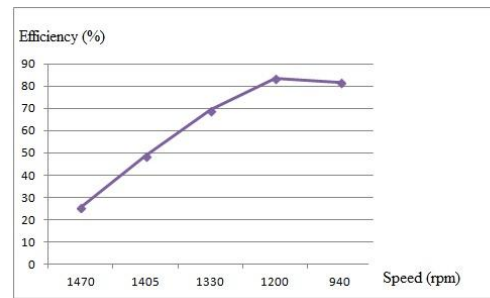
Graph shows that torque increases with decrease in output speed of coupling.

#### 2) Power vs Speed



Graph shows that maximum power is delivered by the coupling at close to 1200 rpm. Thus this is recommended speed at maximum parallel offset condition.

### 3) Efficiency vs Speed



Graph shows that maximum efficiency is attained by the coupling at close to 1200 rpm. Thus this is recommended speed at maximum parallel offset condition for maximum efficiency.

### B) EN-24 Trunion: Angular Offset: 14 Degree Maximum

Aim: To conduct trial and plot

a) Torque vs. Speed Characteristics

b) Power vs. Speed Characteristics

1. Arrangement: In order to conduct trial, a dynobrace pulley cord, weight pan are provided on the output shaft.

2. Procedure:

a) start motor

b) Run mechanism & stabilize at certain speed (say 1500 rpm)

c) Place the pulley cord on dynobrace pulley and add 0.1

Kg weight into the pan, note down the output speed for this load by means of tachometer.

d) Add another 0.2 Kg and take reading.

e) Tabulate the readings in the observation table

f) Plot Torque vs. speed characteristic

g) Power vs. speed characteristic.

### 3. Observation Table

TABLE 16: OBSERVATION TABLE FOR ANGULAR OFFSET

Sr. No	Loading		Unloading		Mean Speed
	Weight (Kg)	Speed rpm	Weight (Kg)	Speed rpm	
1	0.2	1440	2	1420	1430
2	0.4	1320	4	1310	1315
3	0.6	1220	6	1240	1230
4	0.8	1090	8	1080	1070
5	1.0	900	10	880	890

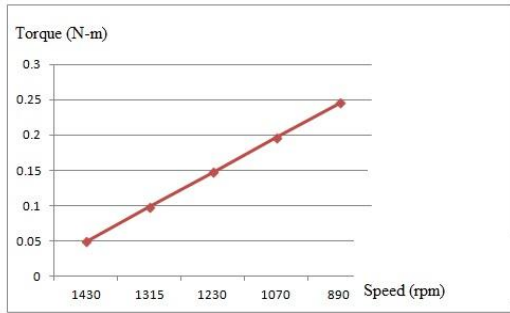
### 4. Result Table

TABLE 17: RESULT TABLE FOR ANGULAR OFFSET

Sr. NO	Load (kg)	Speed (rpm)	Torque (N-m)	Power (watt)	Efficiency (%)
1.	0.2	1430	0.04905	7.346153	24.81808
2.	0.4	1315	0.0981	13.51076	45.64445
3.	0.6	1230	0.14715	18.95616	64.04107
4.	0.8	1070	0.1962	21.98709	74.2807
5.	1.0	890	0.24525	22.86041	77.2311

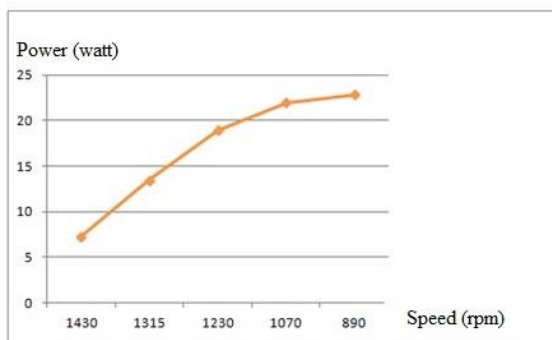
## 5. Characteristics Plots

### 1) Torque vs Speed



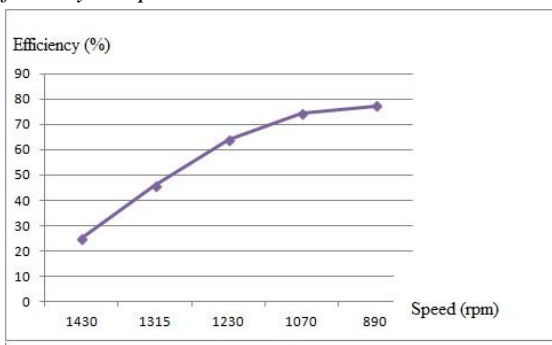
Graph shows that torque increases with decrease in output speed of coupling.

### 2) Power vs Speed



Graph shows that maximum power is delivered by the coupling at close to 900 rpm. Thus this is recommended speed at maximum angular offset condition.

### 3) Efficiency vs Speed



Graph shows that maximum efficiency is attained by the coupling at close to 900 rpm. Thus this is recommended speed at max. angular offset condition for maximum efficiency.

## VI. SCOPE FOR FUTURE WORK

- It is replacement to all present velocity joints.
- One can reduce the cost and space required so that it will easily penetrate in the market.
- Its efficiency can be increased up to 95% by using antifriction material.
- If there are any helix design, that could apply this mechanism.

e) It is remarkable device to be used in industries, plane, helicopters, trains, tractors etc.

## VII. CONCLUSION

Three pin constant velocity joint is replacement to all present velocity joint. One can reduce the cost and space required so that it will easily penetrate in the market. Its efficiency can be increased up to 95% with antifriction material. It has less vibrations and less friction, hence runs cool. It is remarkable device to be used in industries, plane, helicopters, trains, tractors etc. From this project stage 1 on three pin constant velocity joint we will be able to conclude that it is a joint with higher parallel and angular misalignment capability and it can be preferred over universal joint.

Thus we have performed analysis on 3 pin constant velocity joint for parallel and angular power transmission. We have conducted trial on 3 pin constant velocity joint and recorded the readings. We have plotted performance characteristics of the joint such as torque vs speed, power vs speed and efficiency vs speed both for parallel and angular power transmission. From the trial we can conclude that the joint has better performance characteristics than universal joint.

## REFERENCES

- "Design of machine elements", V. B. Bhandari, the McGraw-Hill Companies, 2<sup>nd</sup> edition, 2009.
- "Machine Design Data Book", V. B. Bhandari; McGraw-Hill Publication August 2014.
- "A Textbook of Theory of Machines", Dr. R. K. Bansal, Dr. J. S. Brar, Laxmi Publications (P) LTD, 5<sup>th</sup> edition, October 2011.
- Ian Watson, B. Gangadhara Prusty, John Olsen. Conceptual design optimization of a constant velocity coupling. *Mechanism and Machine Theory* 68 (2013), Page No. 18–34.
- Chul-Hee Lee, Andreas A. Polycarpou. A phenomenological friction model of tripod constant velocity (CV) joints. *Tribology International* 43 (2010) Page No. 844–858.
- Majid Yaghoubi, Seyed Saeid Mohtasebi, Ali Jafary, Hamid Khaleghi. Design, manufacture and evaluation of a new and simple mechanism for transmission of power between intersecting shafts up to 135 degrees (Persian Joint). *Mechanism and Machine Theory* 46 (2011) Page No. 861-868.
- Katsumi Watanabe, Takashi Matsuura. Kinematic Analyses of Rzeppa Constant Velocity Joint by Means of Bilaterally Symmetrical Circular-Arc-Bar Joint.



**Rajkumar Nandkumar Patil** is born on 14 March 1995. He has completed Bachelors of Engineering in mechanical branch at Government College of Engineering and Research, Awasari Kd, Pune affiliated to Savitribai Phule Pune University, Pune.

He has completed many internships through various companies and highly active in social activities.